# Mechanizmy rušení (interference), $f$ > 1 GHz

- 7 základních mechanizmů
- Dlouhodobé
  - působí stále
  - ztráty překročené v min 80 % času

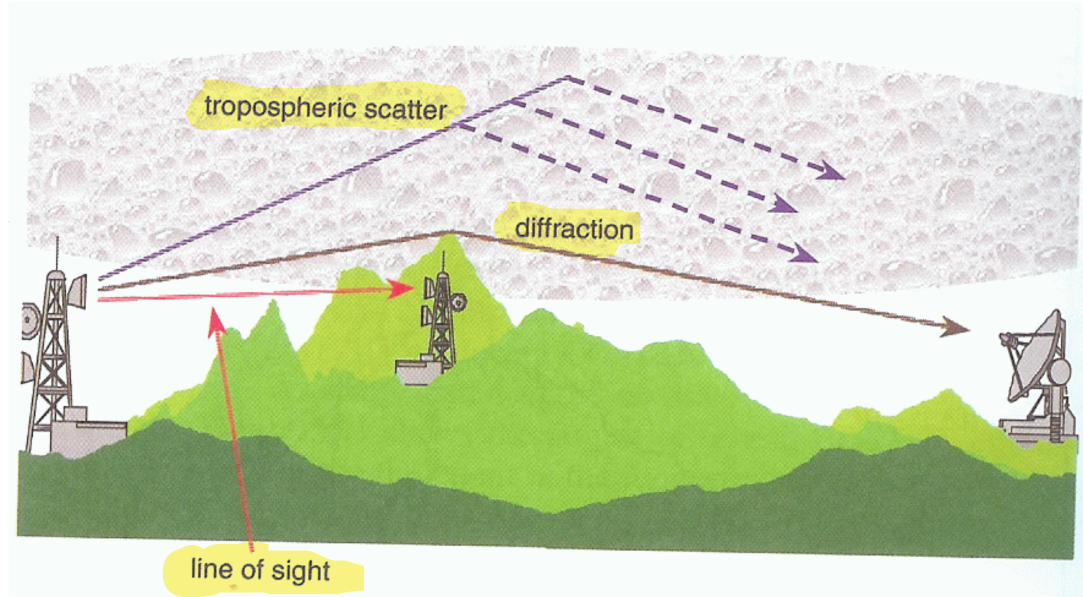


- Krátkodobé
  - anomální stavy
  - Vyskytují se v malém % času

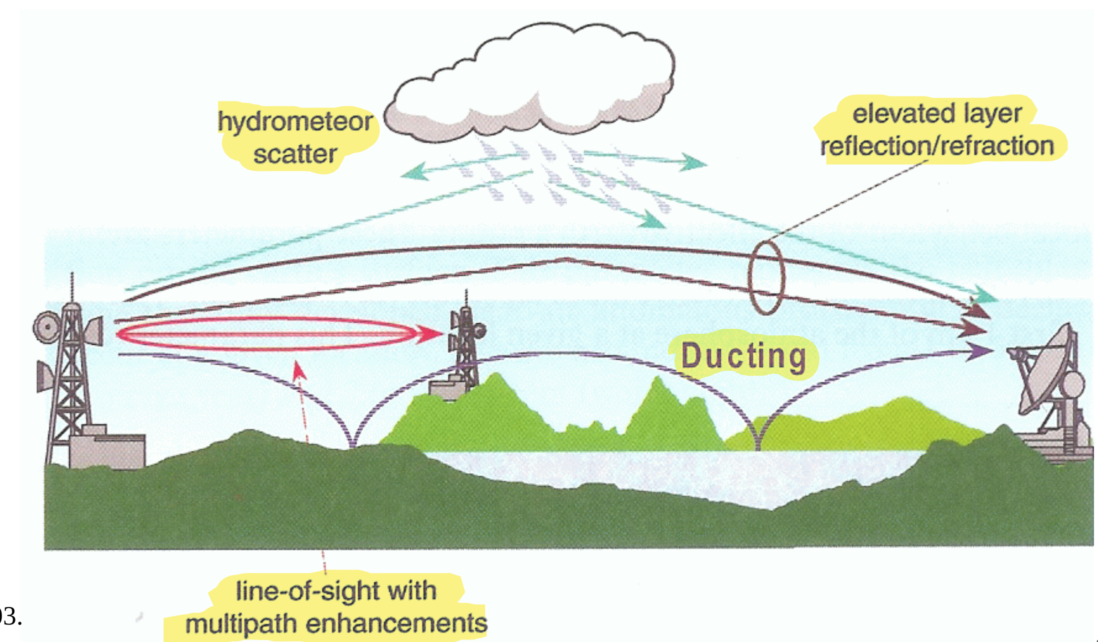


Barclay L.W. (Ed), Propagation of Radiowaves, 2nd edition. IEE, 2003.

# RECOMMENDATION ITU-R P.452-12

## Prediction procedure for the evaluation of microwave interference between stations on the surface of the Earth at frequencies above about 0.7 GHz*

(Question ITU-R 208/3)

(1970-1974-1978-1982-1986-1992-1994-1995-1997-1999-2001-2003-2005)

The ITU Radiocommunication Assembly,

*considering*

a) that due to congestion of the radio spectrum, frequency bands must be shared between different terrestrial services, between systems in the same service and between systems in the terrestrial and Earth-space services;

b) that for the satisfactory coexistence of systems sharing the same frequency bands, interference propagation prediction procedures are needed that are accurate and reliable in operation and acceptable to all parties concerned;

c) that interference propagation predictions are required to meet "worst-month" performance and availability objectives;

d) that prediction methods are required for application to all types of path in all areas of the world,

*recommends*

**1** that the microwave interference prediction procedure given in Annex 1 be used for the evaluation of the available propagation loss in interference calculations between stations on the surface of the Earth for frequencies above about 0.7 GHz.

# Klasifikace základních scénářů

**Interference path classifications and propagation model requirements**

| Classification | Models required |
|---|---|
| Line-of-sight with first Fresnel zone clearance | Line-of-sight (§ 4.2)<br>Clutter loss (§ 4.5, where appropriate) |
| Line-of-sight with sub-path diffraction, i.e. terrain incursion into the first Fresnel zone | Line-of-sight (§ 4.2)<br>Diffraction (§ 4.3)<br>Clutter loss (§ 4.3, where appropriate) |
| Trans-horizon | Diffraction (§ 4.3 for $d \leq 200$ km)<br>Ducting/layer reflection (§ 4.5)<br>Troposcatter (§ 4.4)<br>Clutter loss (§ 4.6, where appropriate) |

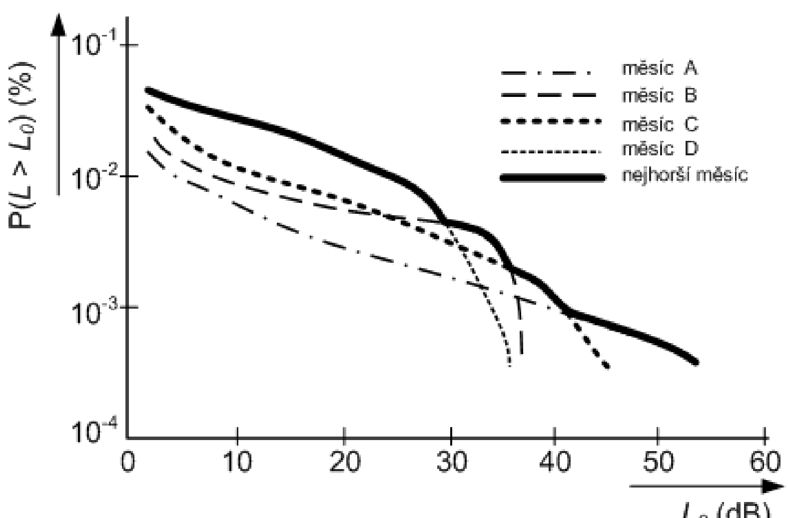

## Methods of deriving overall predictions

| Path type | Action required |
|---|---|
| Line-of-sight | The prediction is obtained by summing the losses given by the line-of-sight and clutter loss models, i.e.:<br>$L_b\,(p) = L_{b0}\,(p) + A_{ht} + A_{hr}$ dB (8a)<br>where:<br>$L_{b0}\,(p)$ : predicted basic transmission loss not exceeded for $p$% of time given by the line-of-sight model<br>$A_{ht}$, $A_{hr}$ : appropriate additional losses due to height-gain effects in local clutter |
| Line-of-sight with sub-path diffraction | The prediction is obtained by summing the losses given by the line-of-sight and (sub-path) diffraction models and clutter models, i.e.:<br>$L_b\,(p) = L_{b0}\,(p) + L_{ds}\,(p) + A_{ht} + A_{hr}$ dB (8b)<br>where:<br>$L_{ds}\,(p)$: prediction for $p$% of time given by the sub-path diffraction loss element of the diffraction model |
| Trans-horizon | The overall prediction is obtained in three stages:<br>The unmodified ducting/layer reflection loss $L_{ba}$ is obtained using the method in § 4.5.<br>The modified ducting/layer reflection model loss, $L_{bam}(p)$, is found by application of the algorithm in § 4.7.1.<br>The overall prediction can then be obtained by applying the following ancillary algorithm:<br>$L_b(p) - 5\log\left(10^{-0.2L_{bs}} + 10^{-0.2L_{bd}} + 10^{-0.2L_{bam}}\right) + A_{ht} + A_{hr}$ dB (8c)<br>where $L_{bs}\,(p)$ and $L_{bd}\,(p)$: individual predicted basic transmission loss for $p$% of time given by the troposcatter and diffraction propagation models respectively.<br>NOTE 1 – Where a model has not been proposed for a path (because the conditions given in Table 4 were not met), the appropriate term should be omitted from equation (8c). |

### 4.2 Line-of-sight propagation (including short-term effects)

The basic transmission loss $L_{b0}(p)$ not exceeded for time percentage, $p$%, due to line-of-sight propagation is given by:

$$L_{b0}(p) = 92.5 + 20 \log f + 20 \log d + E_s(p) + A_g \qquad \text{dB} \qquad (9)$$

where:

$E_s(p)$: correction for multipath and focusing effects:

$$E_s(p) = 2.6\,(1 - e^{-d/10}) \log (p / 50) \qquad \text{dB} \qquad (10)$$

$A_g$: total gaseous absorption (dB):

$$A_g = [\gamma_o + \gamma_w(\rho)]\, d \qquad \text{dB} \qquad (11)$$

where:

$\gamma_o$, $\gamma_w(\rho)$: specific attenuation due to dry air and water vapour, respectively, and are found from the equations in Recommendation ITU-R P.676

$\rho$: water vapour density:

$$\rho = 7.5 + 2.5\,\omega \qquad \text{g/m}^3$$

$\omega$: fraction of the total path over water.

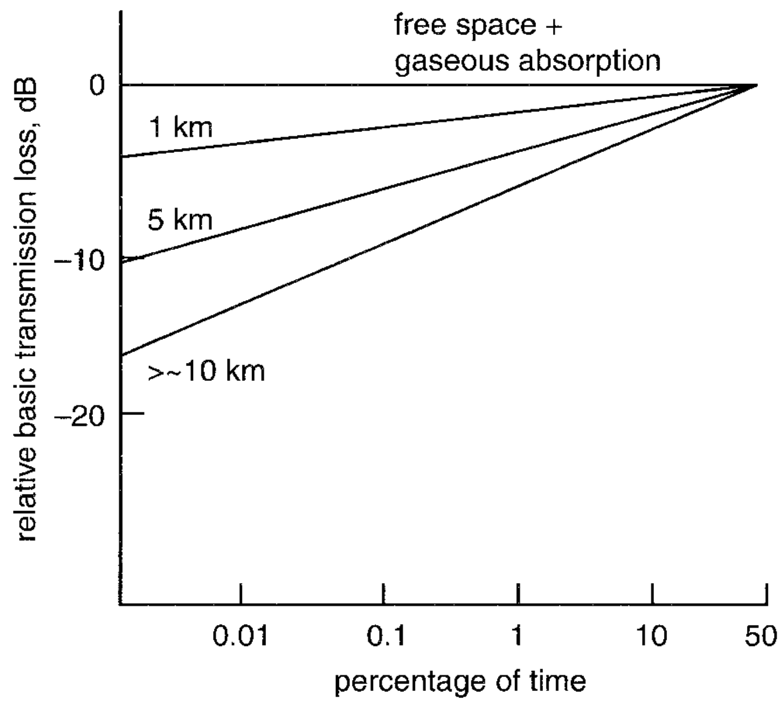


*Reduced line-of-sight loss due to multipath effects*

Barclay L.W. (Ed), Propagation of Radiowaves, 2nd edition. IEE, 2003.

### 4.6.3 The height-gain model

The additional loss due to protection from local clutter is given by the expression:

$$A_h = 10.25 \times e^{-d_k} \left( 1 - \tanh\left[ 6 \left( \frac{h}{h_a} - 0.625 \right) \right] \right) - 0.33 \qquad \text{dB}$$

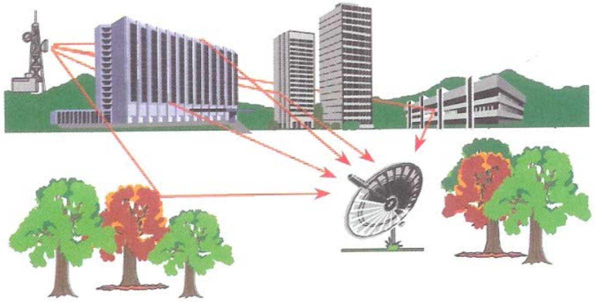

where:

- $d_k$: distance (km) from nominal clutter point to the antenna (see Fig. 3)
- $h$: antenna height (m) above local ground level
- $h_a$: nominal clutter height (m) above local ground level.

**Method of applying height-gain correction, $A_{ht}$ or $A_{hr}$**

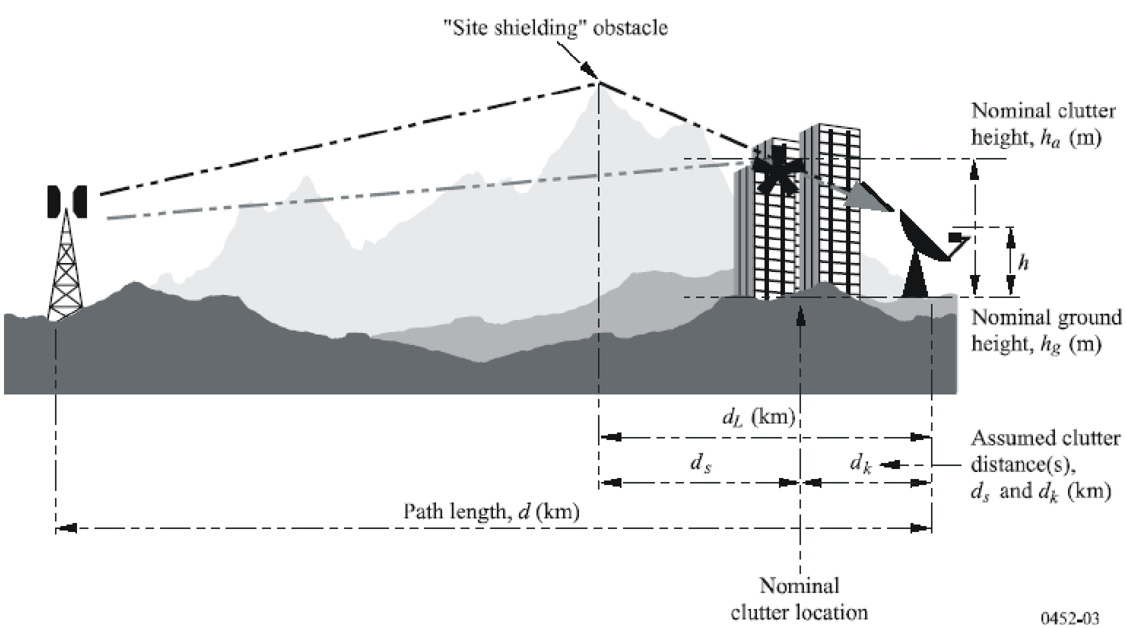


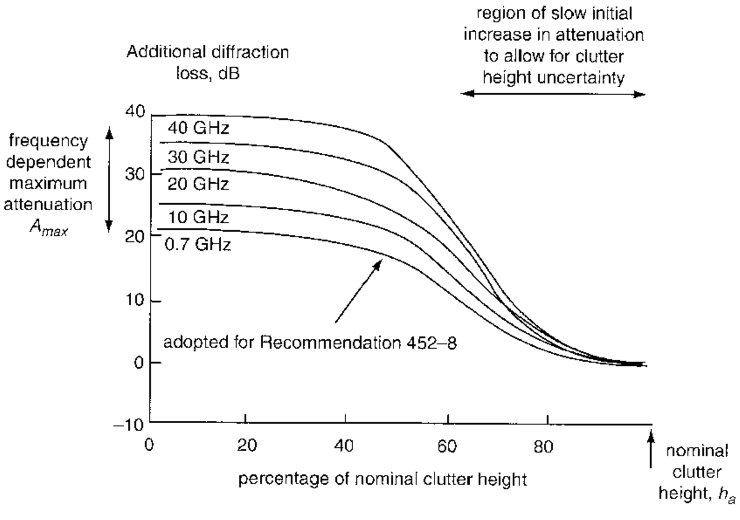


Barclay L.W. (Ed), Propagation of Radiowaves, 2nd edition. IEE, 2003.

## Nominal clutter heights and distances

| Clutter (ground-cover) category | Nominal height, $h_a$ (m) | Nominal distance, $d_k$ (km) |
|---|---|---|
| High crop fields<br>Park land<br>Irregularly spaced sparse trees<br>Orchard (regularly spaced)<br>Sparse houses | 4 | 0.1 |
| Village centre | 5 | 0.07 |
| Deciduous trees (irregularly spaced)<br>Deciduous trees (regularly spaced)<br>Mixed tree forest | 15 | 0.05 |
| Coniferous trees (irregularly spaced)<br>Coniferous trees (regularly spaced) | 20 | 0.05 |
| Tropical rain forest | 20 | 0.03 |
| Suburban | 9 | 0.025 |
| Dense suburban | 12 | 0.02 |
| Urban | 20 | 0.02 |
| Dense urban | 25 | 0.02 |
| Industrial zone | 20 | 0.05 |

**Method of applying height-gain correction, $A_{ht}$ or $A_{hr}$**

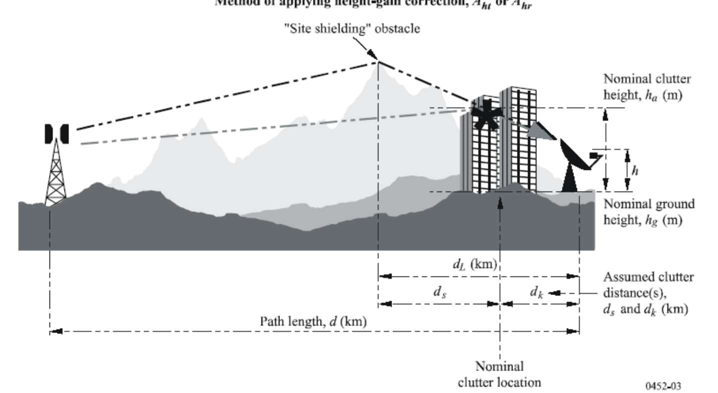

# Difrakce - vliv refrakce -> efektivní poloměr Země

a)

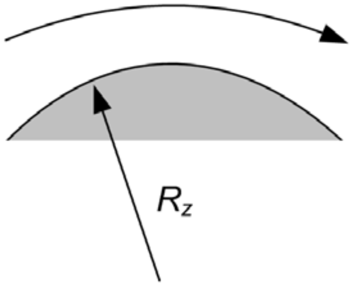


b)

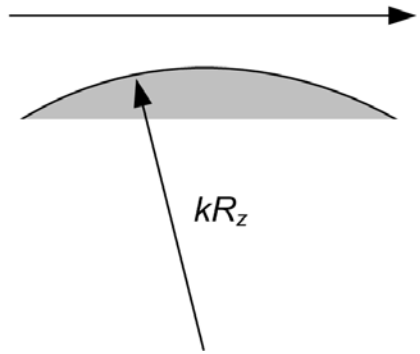


$$\frac{1}{R_\mathrm{z}} - \frac{1}{R_\mathrm{k}} = \frac{1}{R_\mathrm{e}} - \frac{1}{\infty}$$

$$R_\mathrm{e} = \frac{R_\mathrm{z}}{1 - \dfrac{R_\mathrm{z}}{R_\mathrm{k}}} = k_e R_\mathrm{z}$$

$$k_\mathrm{e} = \frac{R_\mathrm{e}}{R_\mathrm{z}} = \frac{1}{1 + R_\mathrm{z} \dfrac{\mathrm{d}N}{\mathrm{d}h} 10^{-6}}$$

$$= \frac{157}{157 - |\Delta N|}$$

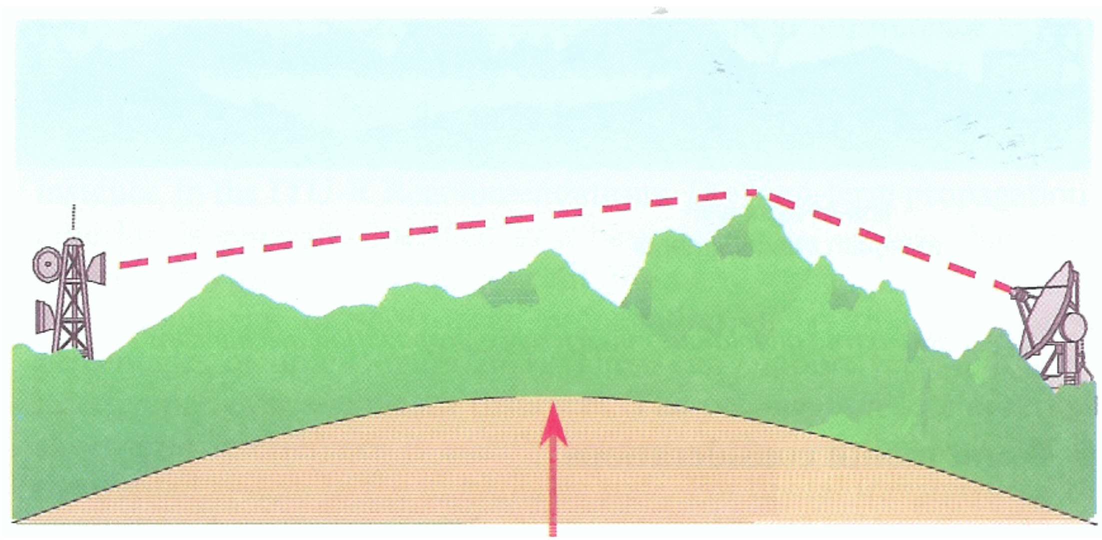

$\Delta N$ (N-units/km), the average radio-refractive index lapse-rate through the lowest 1 km of the atmosphere, provides the data upon which the appropriate effective Earth radius can be calculated for path profile and diffraction obstacle analysis. Figures 11 and 12, respectively, provide world maps of average annual $\Delta N$ values and maximum monthly mean values for worst-month predictions. Note that $\Delta N$ is a positive quantity in this procedure.

FIGURE 11

**Average annual values of $\Delta N$**

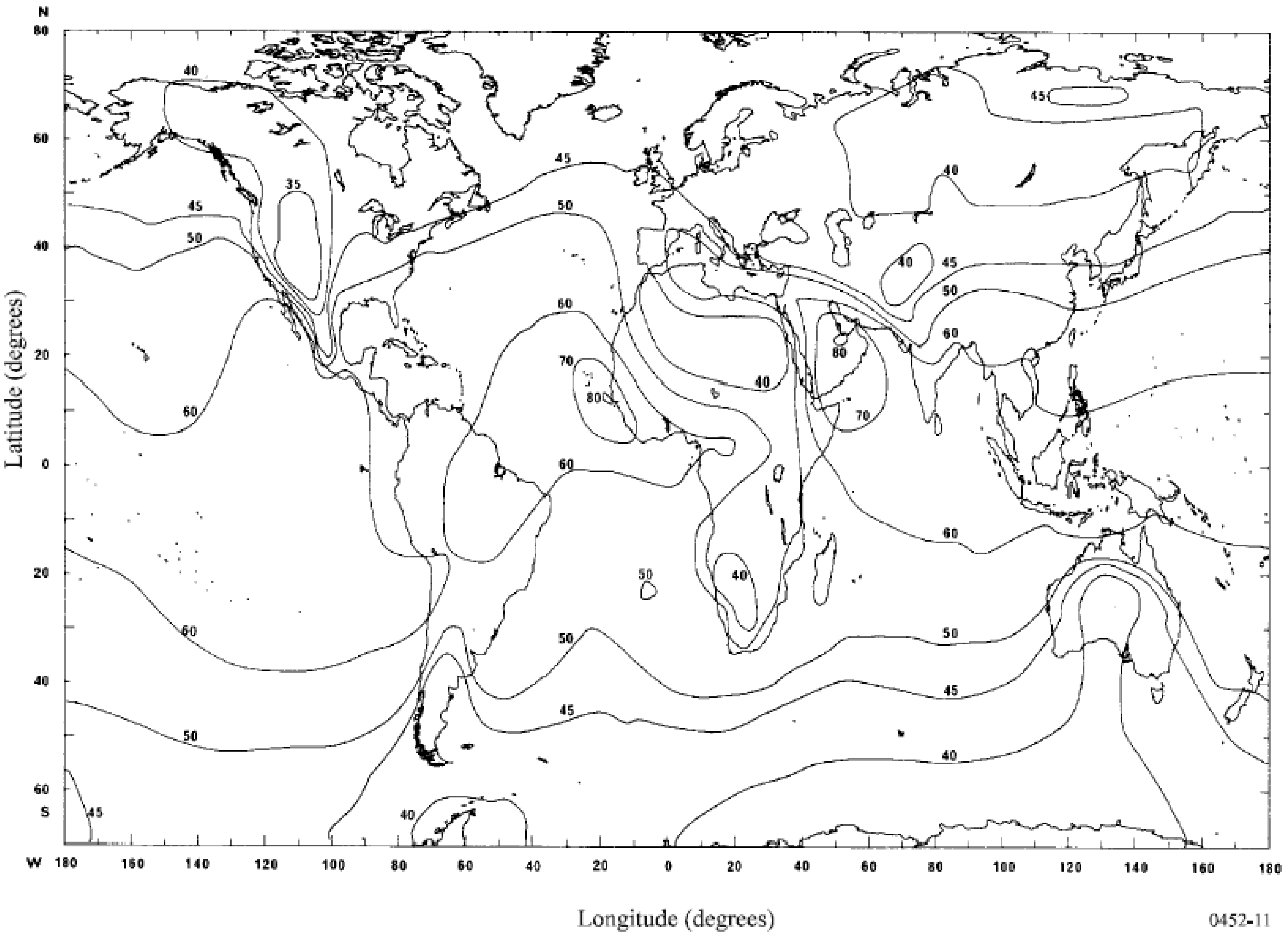


0452-11

30 – 80 N/km

FIGURE 12

**Maximum monthly mean values of ΔN (for worst-month prediction)**

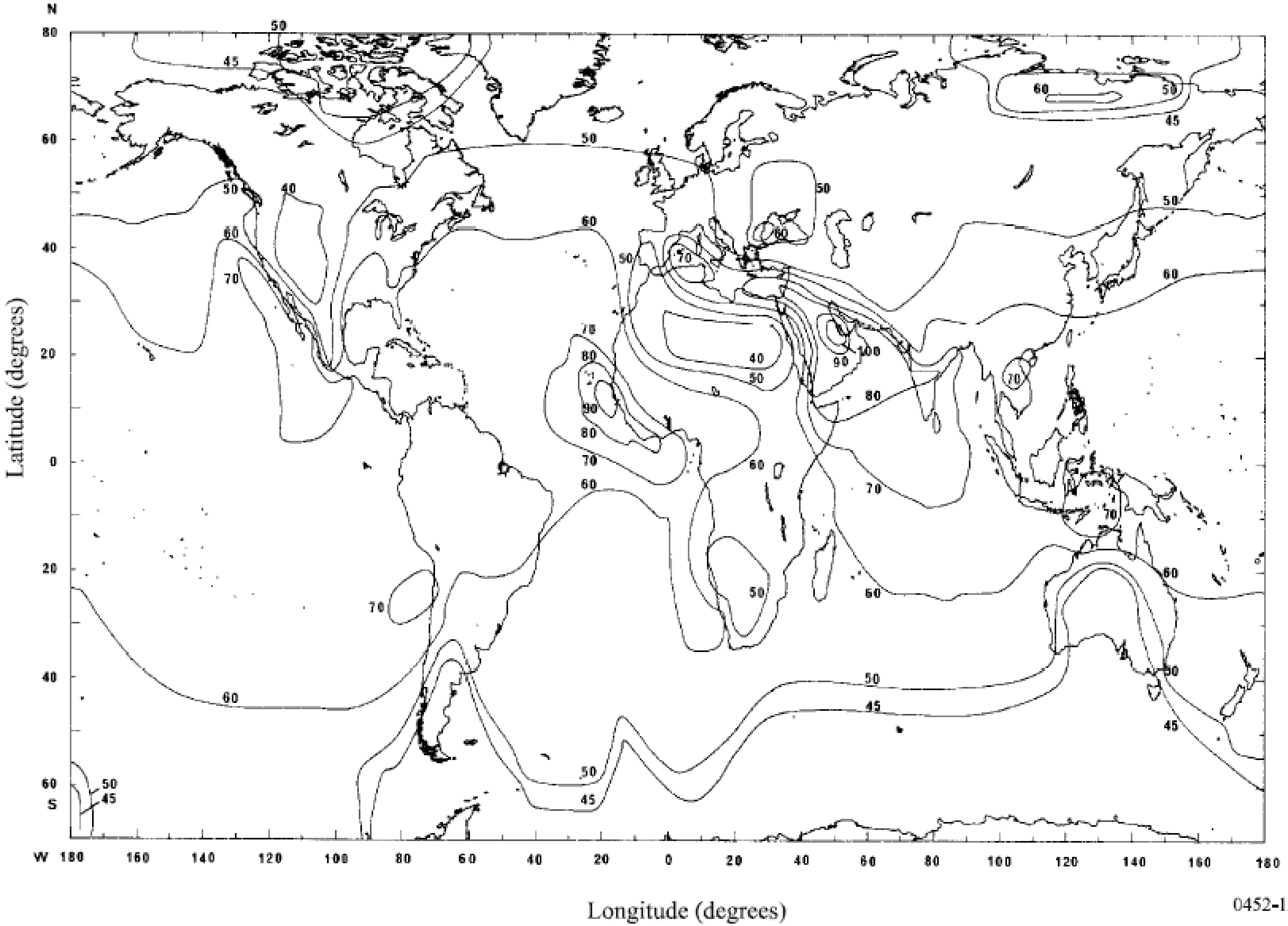


50 – 100 N/km

# Statistika činitele atmosférické refrakce

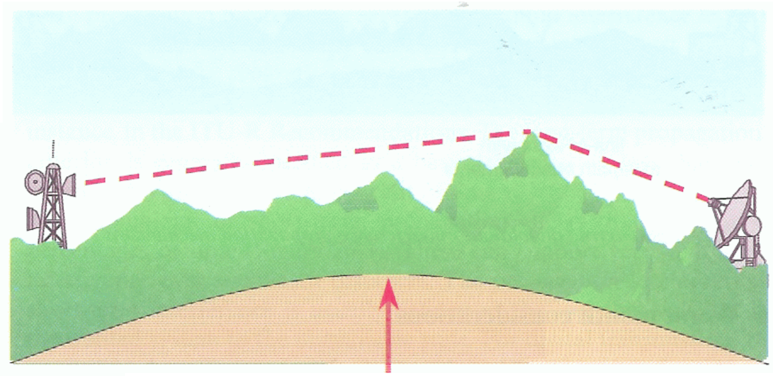

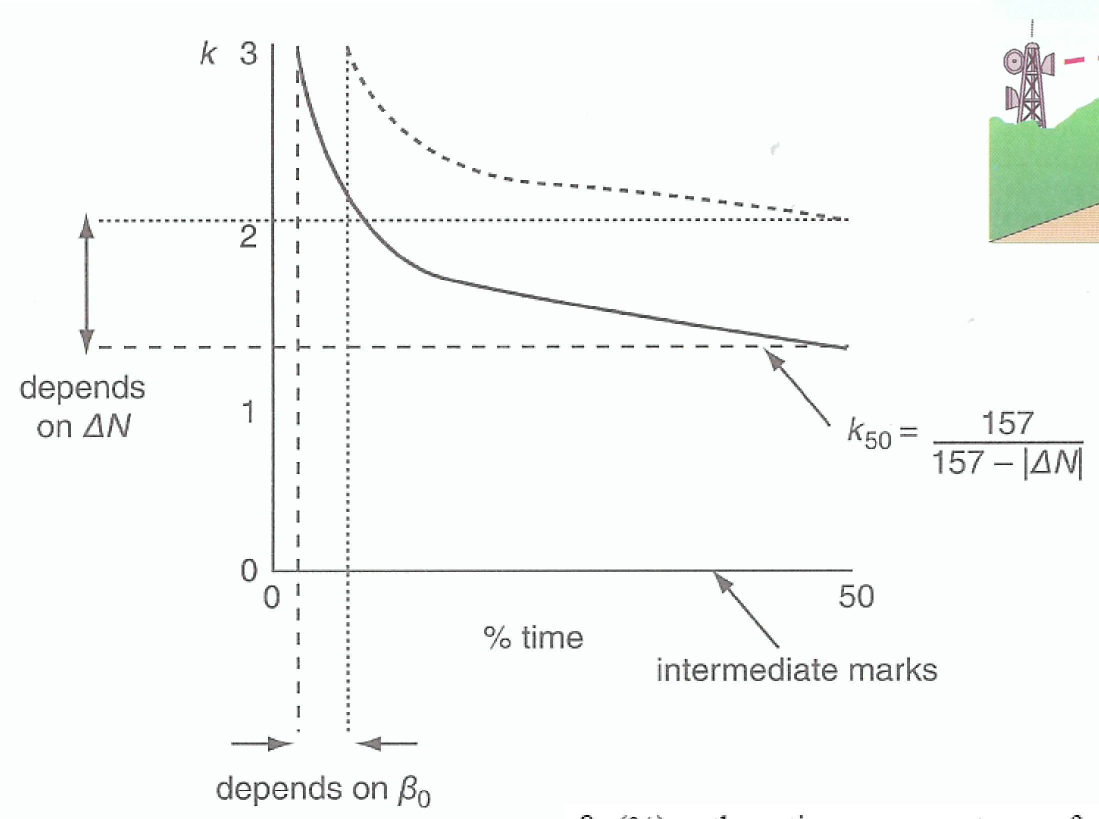


$\beta_0$ (%), the time percentage for which refractive index lapse-rates exceeding 100 N-units/km can be expected in the first 100 m of the lower atmosphere, is used to estimate the relative incidence of fully developed anomalous propagation at the latitude under consideration. The value of $\beta_0$ to be used is that appropriate to the path centre latitude.

průměrný rok: 1 – 50 %
nejhorší měsíc: 2 – 90 %

Barclay L.W. (Ed), Propagation of Radiowaves, 2nd edition. IEE, 2003.

## 4.3 Diffraction

The time variability of the excess loss due to the diffraction mechanism is assumed to be the result of changes in bulk atmospheric radio refractivity lapse rate, i.e. as the time percentage $p$ reduces, the effective Earth radius factor $k(p)$ is assumed to increase. This process is considered valid for $\beta_0 \leq p \leq 50\%$. For time percentages less than $\beta_0$ signal levels are dominated by anomalous propagation mechanisms rather than by the bulk refractivity characteristics of the atmosphere. Thus for values of $p$ less than $\beta_0$ the value of $k(p)$ has the value $k(\beta_0)$.

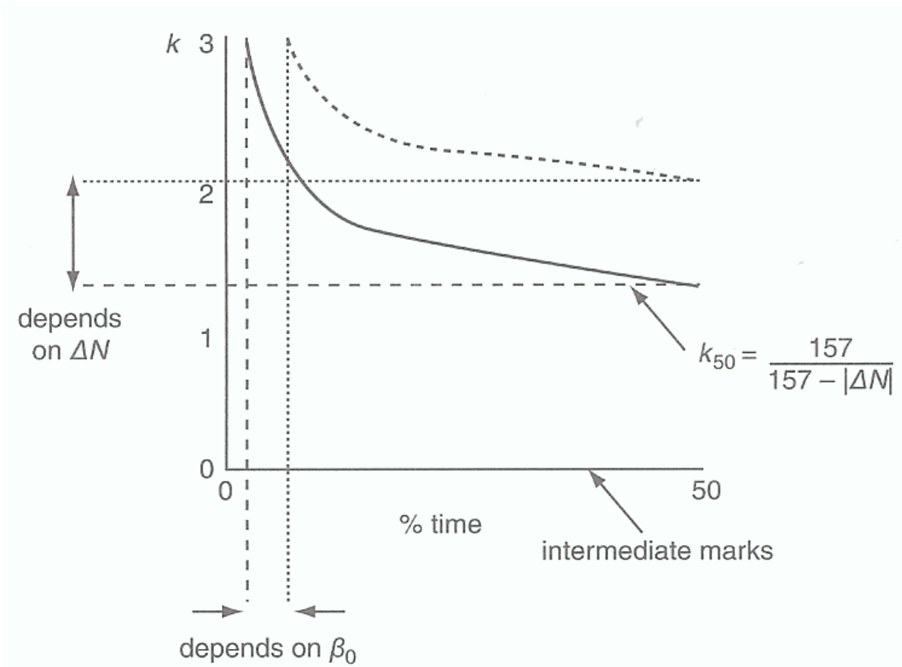


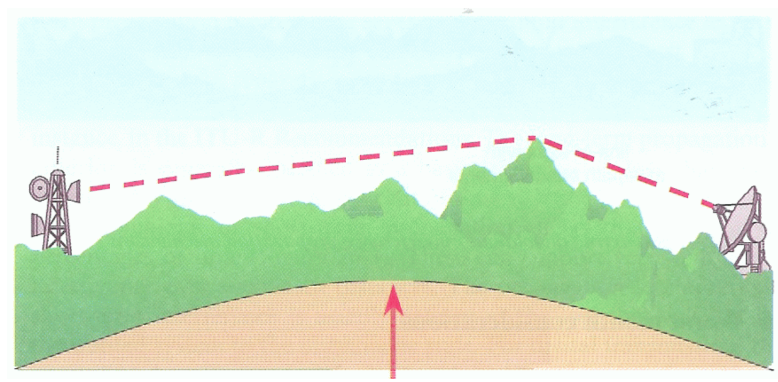

Deygout:

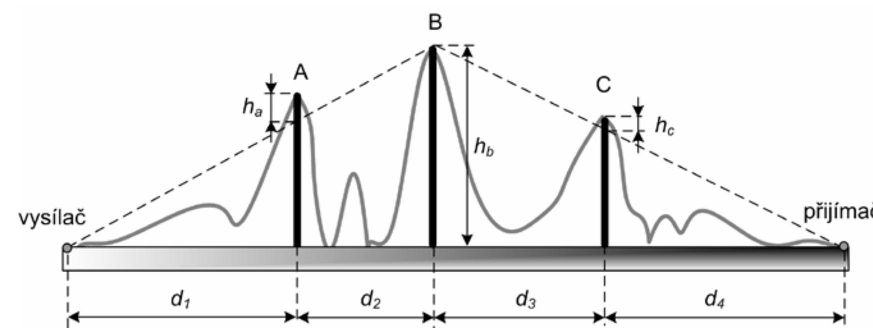

# Vliv konkrétního terénního profilu

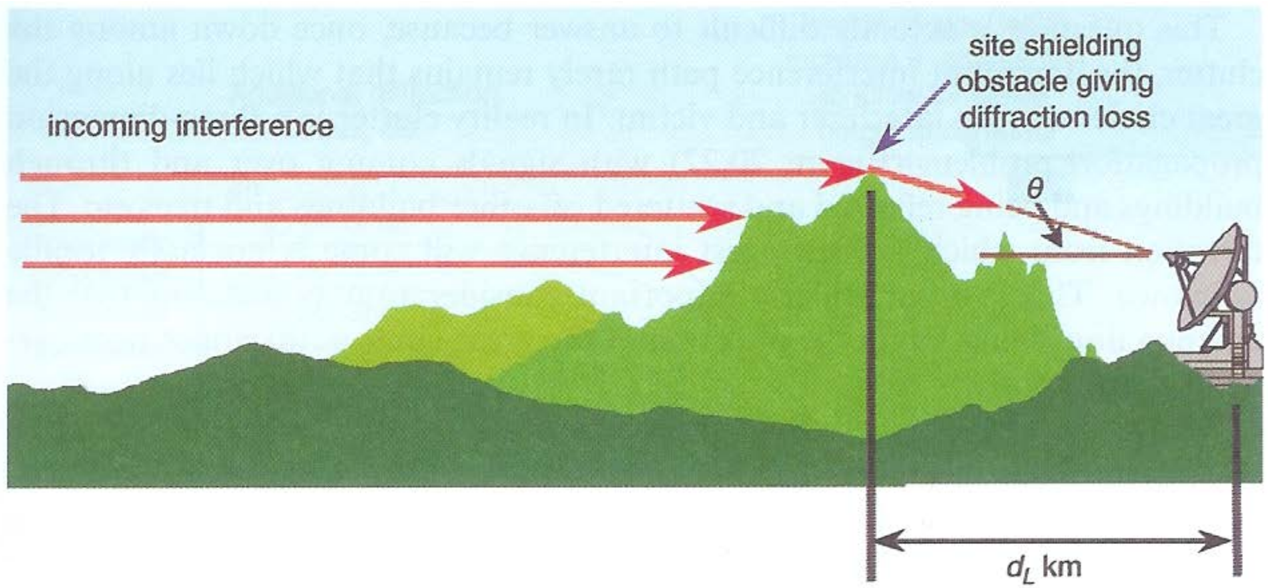


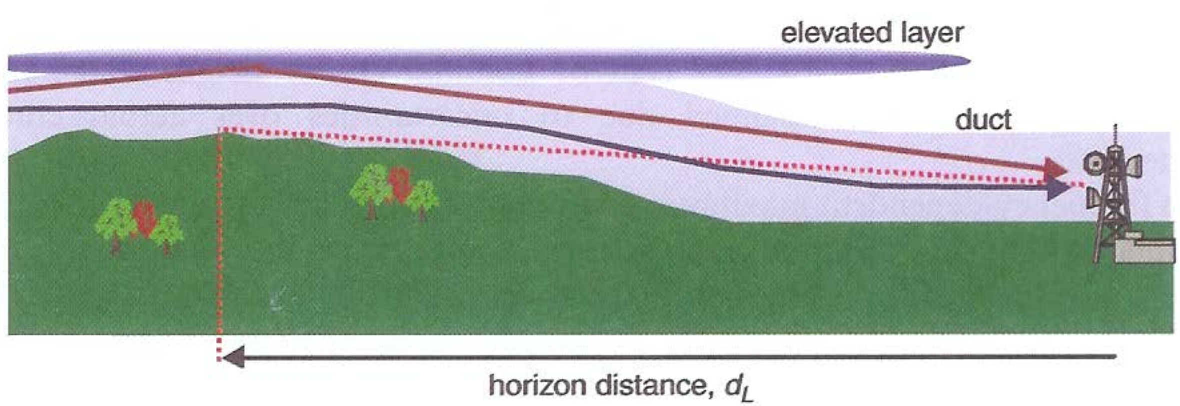


Barclay L.W. (Ed), Propagation of Radiowaves, 2nd edition. IEE, 2003.

# Klasifikace základních scénářů

**Interference path classifications and propagation model requirements**

| Classification | Models required |
|---|---|
| Line-of-sight with first Fresnel zone clearance | Line-of-sight (§ 4.2)<br>Clutter loss (§ 4.5, where appropriate) |
| Line-of-sight with sub-path diffraction, i.e. terrain incursion into the first Fresnel zone | Line-of-sight (§ 4.2)<br>Diffraction (§ 4.3)<br>Clutter loss (§ 4.3, where appropriate) |
| Trans-horizon | Diffraction (§ 4.3 for $d \leq 200$ km)<br>Ducting/layer reflection (§ 4.5)<br>Troposcatter (§ 4.4)<br>Clutter loss (§ 4.6, where appropriate) |

# Troposférický rozptyl

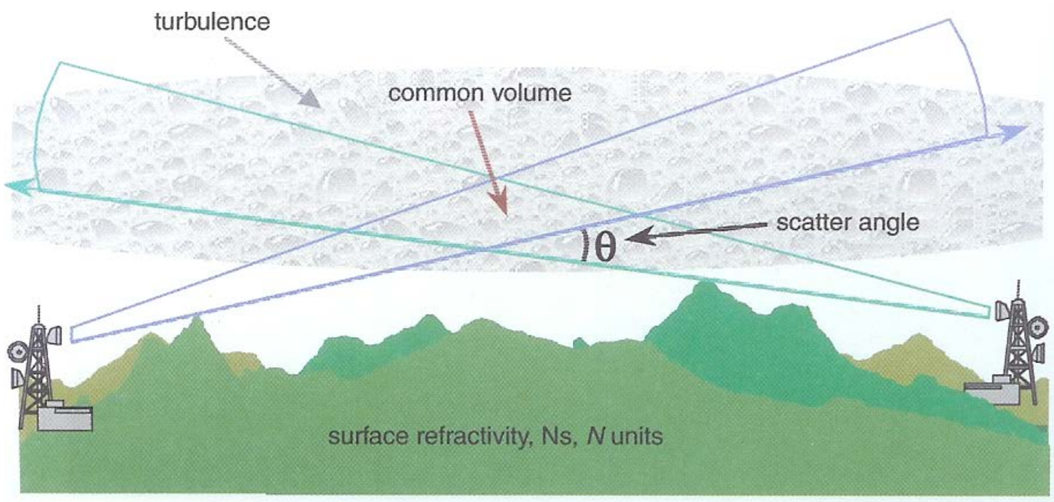


$N_0$ (N-units), the sea-level surface refractivity, is used only by the troposcatter model as a measure of location variability of the troposcatter scatter mechanism. Figure 13 provides annual values of $N_0$. As the scatter path calculation is based on a path geometry determined by annual or worst-month values of $\Delta N$, there is no additional need for worst-month values of $N_0$. The correct values of $\Delta N$ and $N_0$ are given by the path-centre values as derived from the appropriate maps.

FIGURE 13

Sea-level surface refractivity, $N_0$

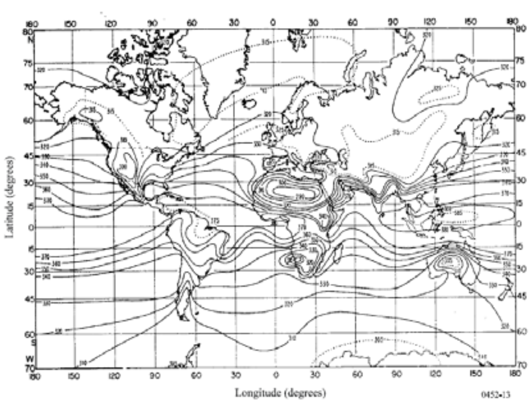


Barclay L.W. (Ed), Propagation of Radiowaves, 2nd edition. IEE, 2003.

FIGURE 13

**Sea-level surface refractivity, $N_0$**

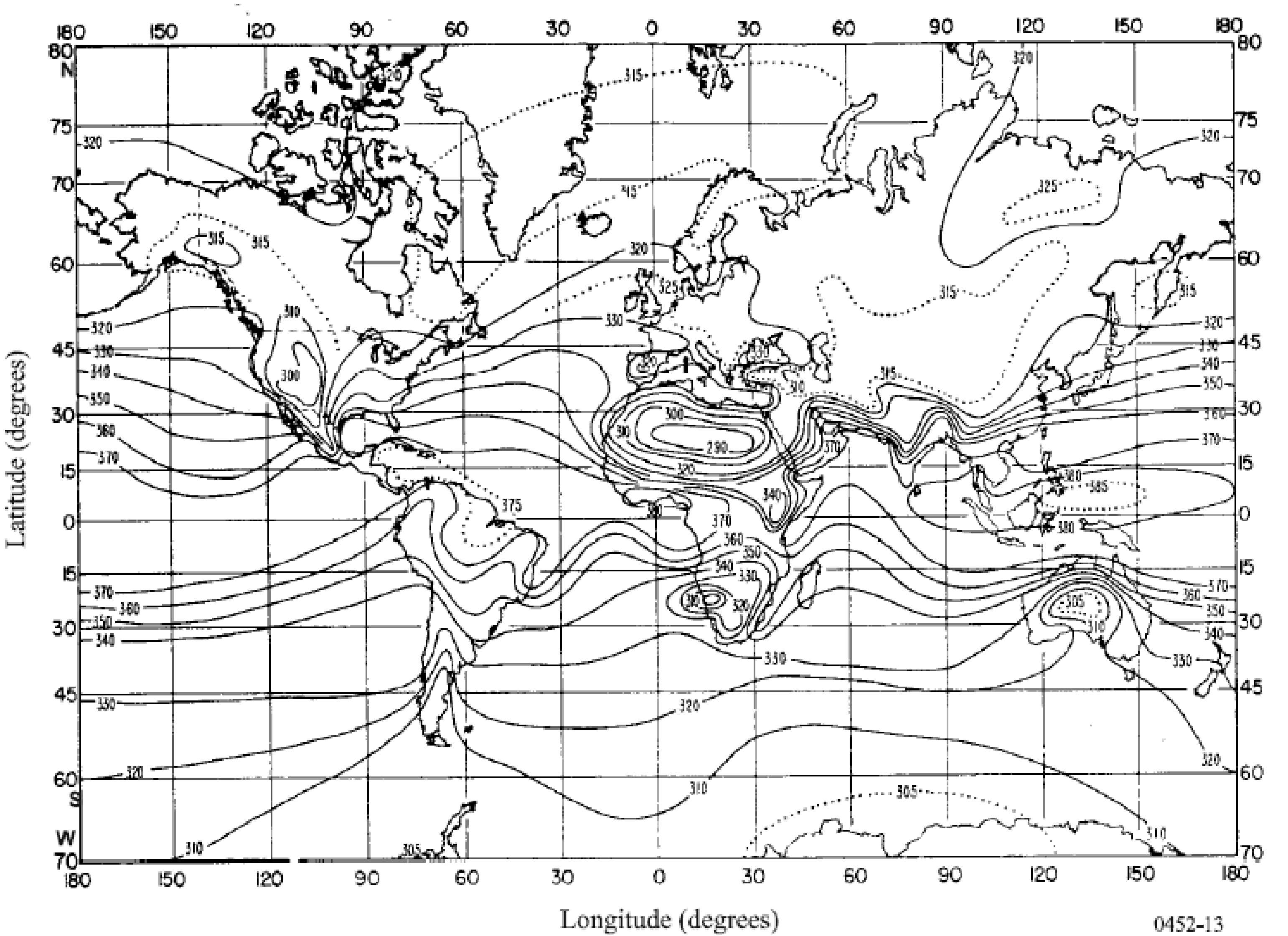

# Šíření vlnovodným kanálem (*ducting*) Odraz/refrakce na vyvýšené vrstvě troposféry

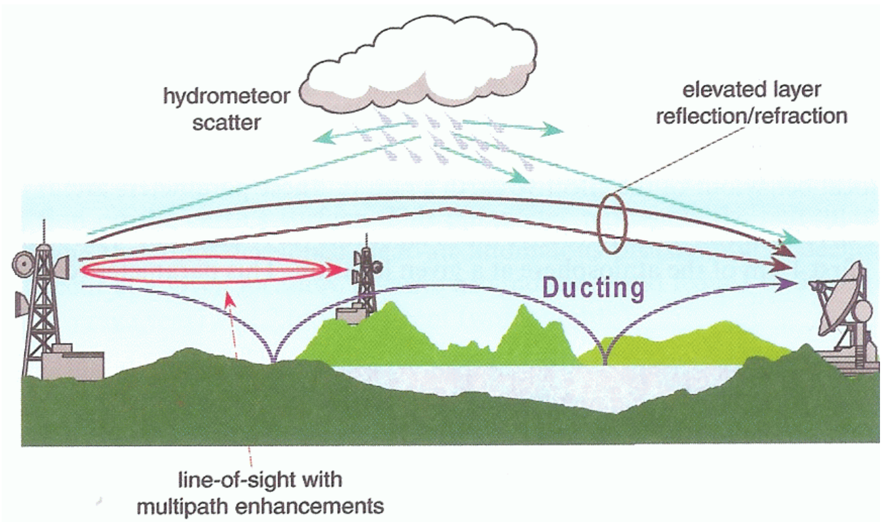


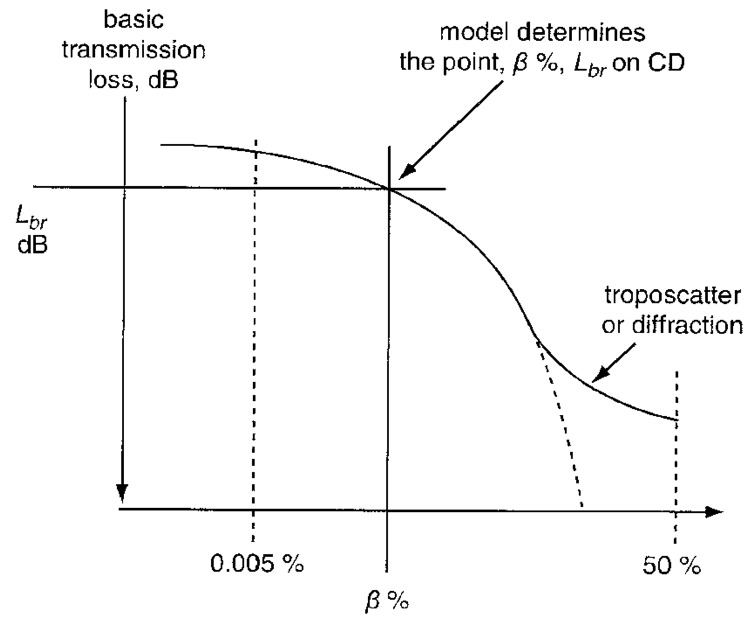


*Basic approach used for the anomalous propagation*

- Stanovení příslušného časového procenta $\beta$
  - Vychází z parametru $\beta_0$ korigovaného na příslušnou situaci (4 faktory)
    - vnitrozemí / pobřežní oblasti / nad mořem
    - konkrétní geometrie trasy
    - drsnost terénu
    - geografická poloha

$$\beta = \beta_0 \mu_1 \mu_2 \mu_3 \mu_4 \quad \% \text{ času}$$

- Stanovení odpovídajících ztrát šířením, které nejsou překročeny v $\beta$ času

# vnitrozemí / pobřežní oblast / nad mořem

$$\beta = \beta_0 \mu_1 \mu_2 \mu_3 \mu_4 \quad \% \text{ času}$$

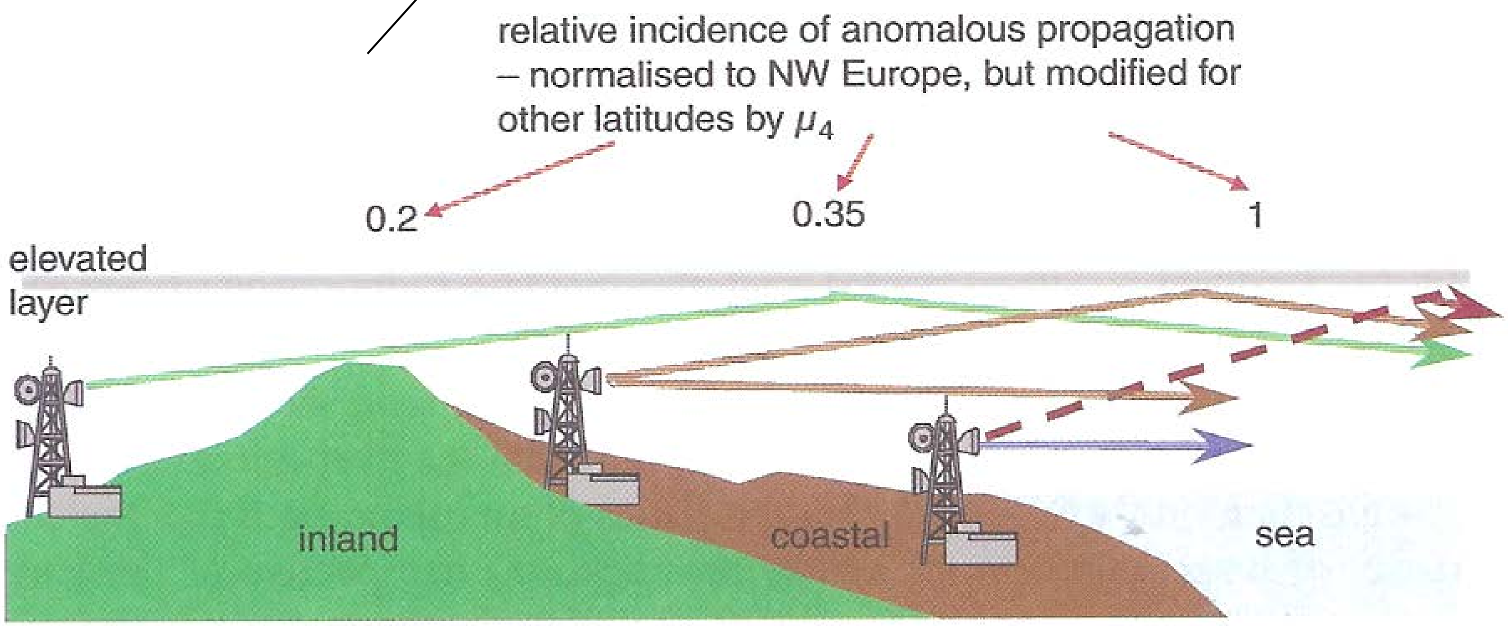


*Relative incidence of anomalous propagation over inland, sea and coastal areas (values shown are for NW Europe)*

Barclay L.W. (Ed), Propagation of Radiowaves, 2nd edition. IEE, 2003.

# Vliv geometrie

$$\beta = \beta_0 \mu_1 \mu_2 \mu_3 \mu_4 \quad \text{% času}$$

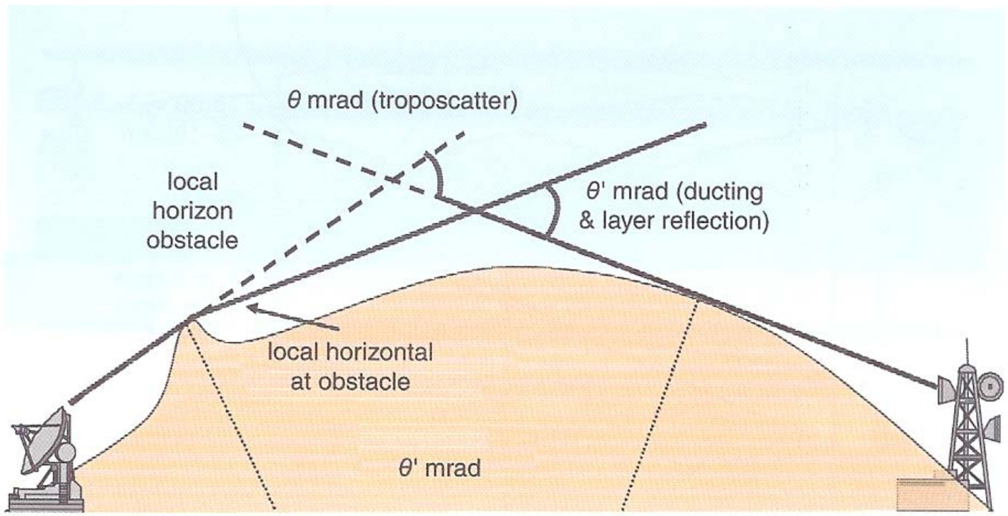


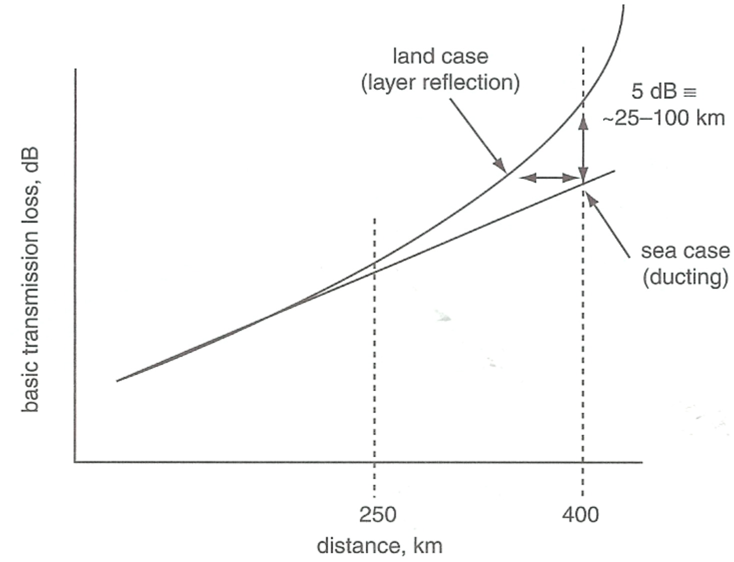


- Z rostoucím úhlem rozptylu klesá pravděpodobnost anomálního šíření
- Pro menší vzdálenosti (do cca 250 km) mají oba mechanizmy (vlnovodný kanál a odraz/refrakce na vyvýšené vrstvě) podobný dopad (podobné ztráty šířením)
- Pro větší vzdálenosti klesá pravděpodobnost odrazu/refrakce na vyvýšené vrstvě = vyšší ztráty; vlnovodný kanál se naopak může uplatnit pro vzdálenosti až 1000 km

Barclay L.W. (Ed), Propagation of Radiowaves, 2nd edition. IEE, 2003.

# Vliv drsnosti terénu

$$\beta = \beta_0 \mu_1 \mu_2 \mu_3 \mu_4 \quad \% \text{ času}$$

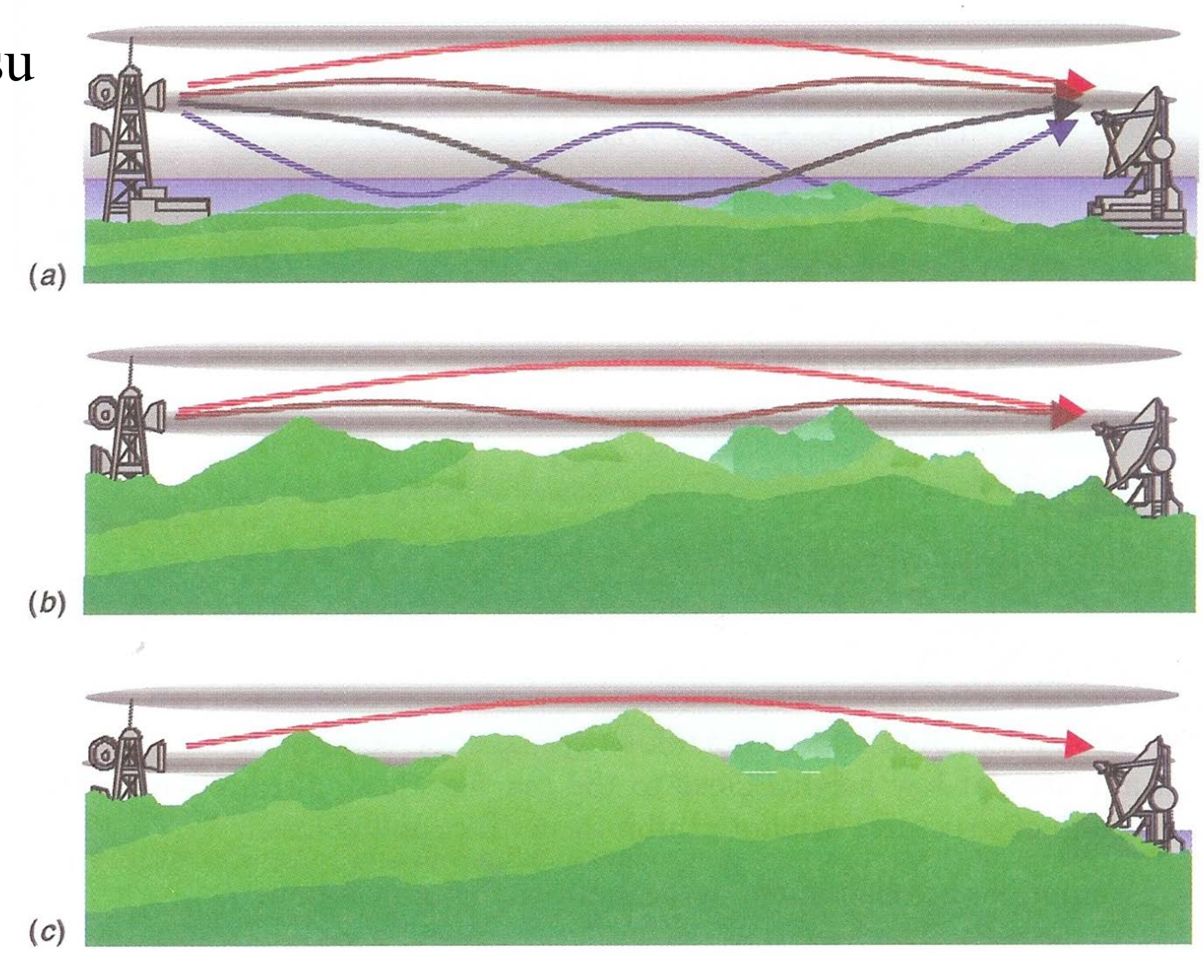

Figure 20.16 The impact of increasing terrain roughness
(a) flat terrain – high probability of interference
(b) rough terrain – less probability of interference
(c) rugged terrain – low probability of interference

Barclay L.W. (Ed), Propagation of Radiowaves, 2nd edition. IEE, 2003.

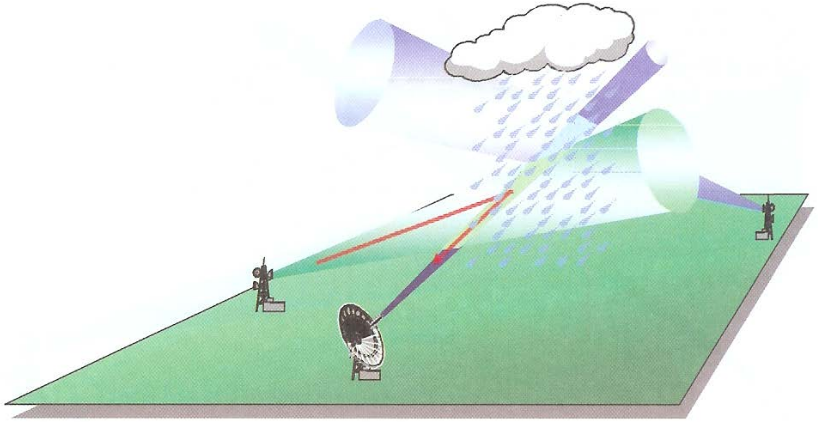

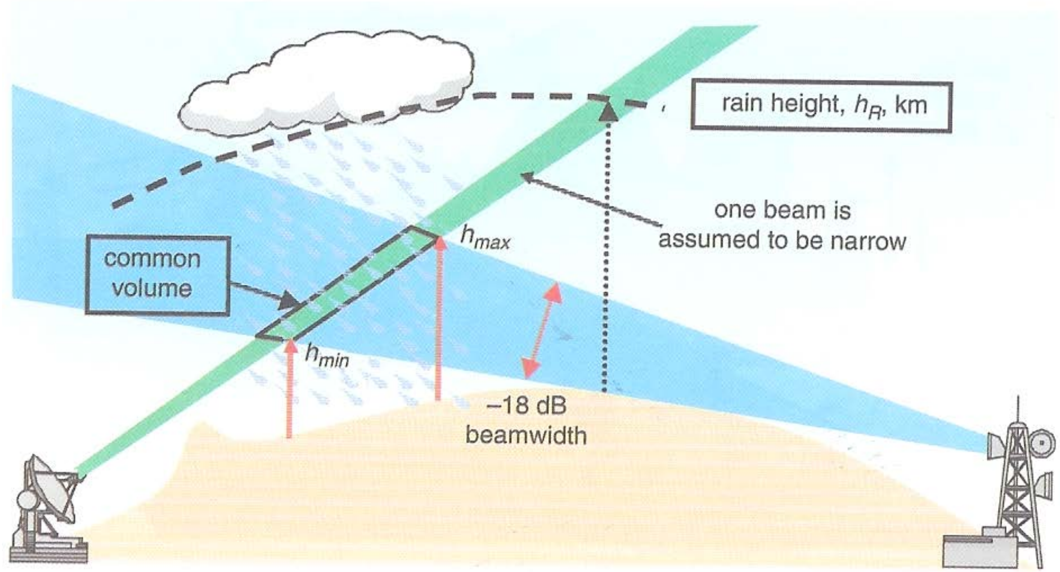


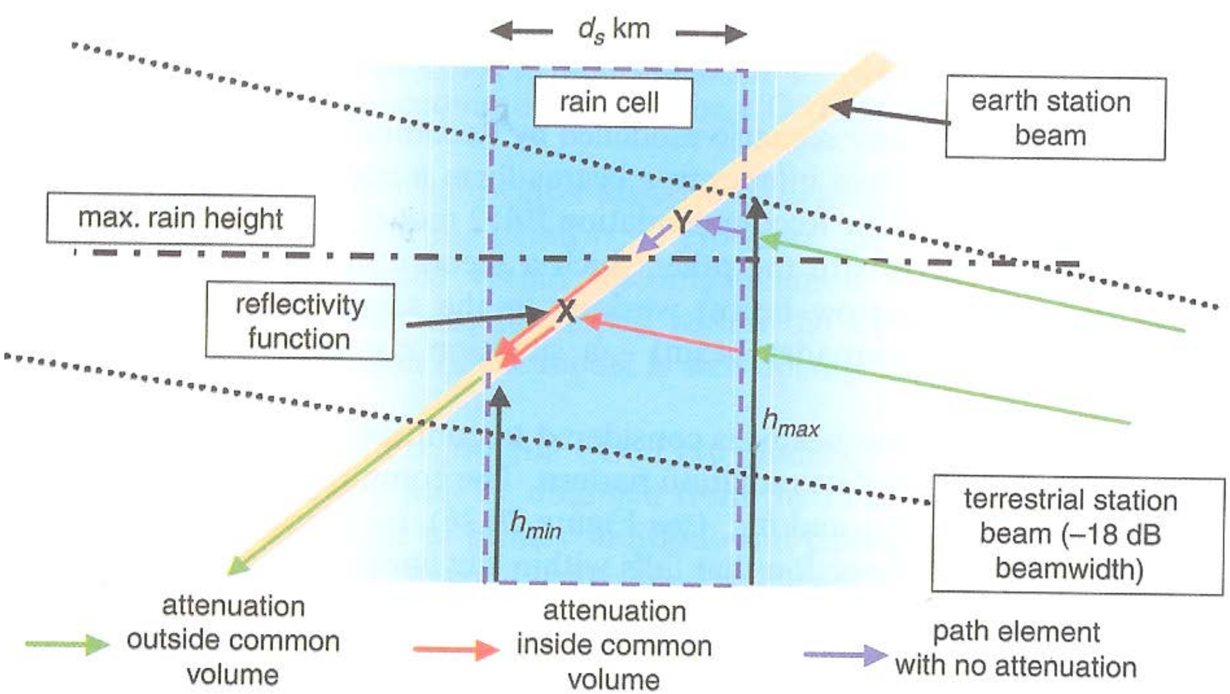


Barclay L.W. (Ed), Propagation of Radiowaves, 2nd edition. IEE, 2003.

# Výsledek

= „obálka" distribučních funkcí pro jednotlivé mechanizmy
= pro každé procento času nejmenší ztráty šířením (které nejsou v daném % času překročeny)

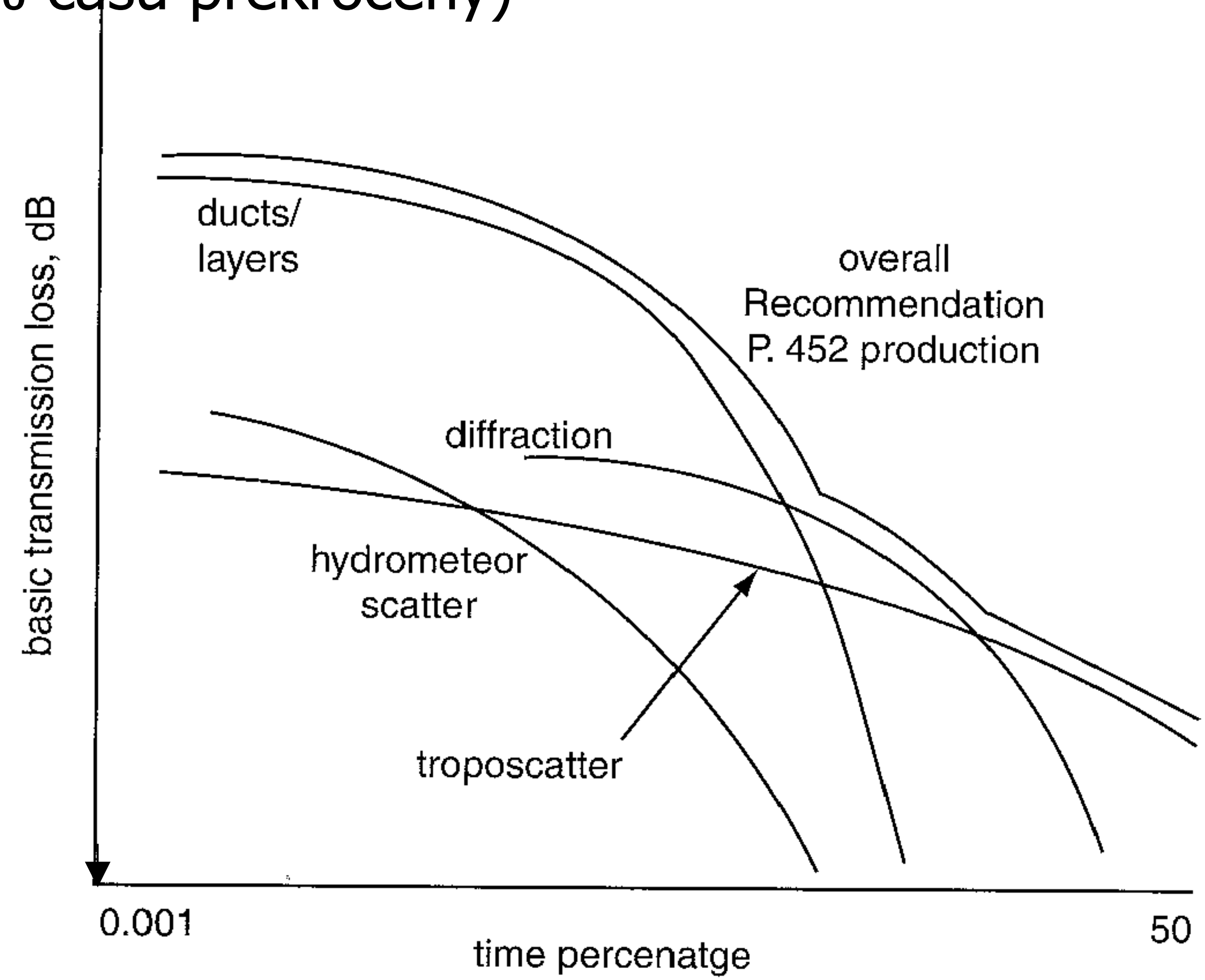


Barclay L.W. (Ed), Propagation of Radiowaves, 2nd edition. IEE, 2003.

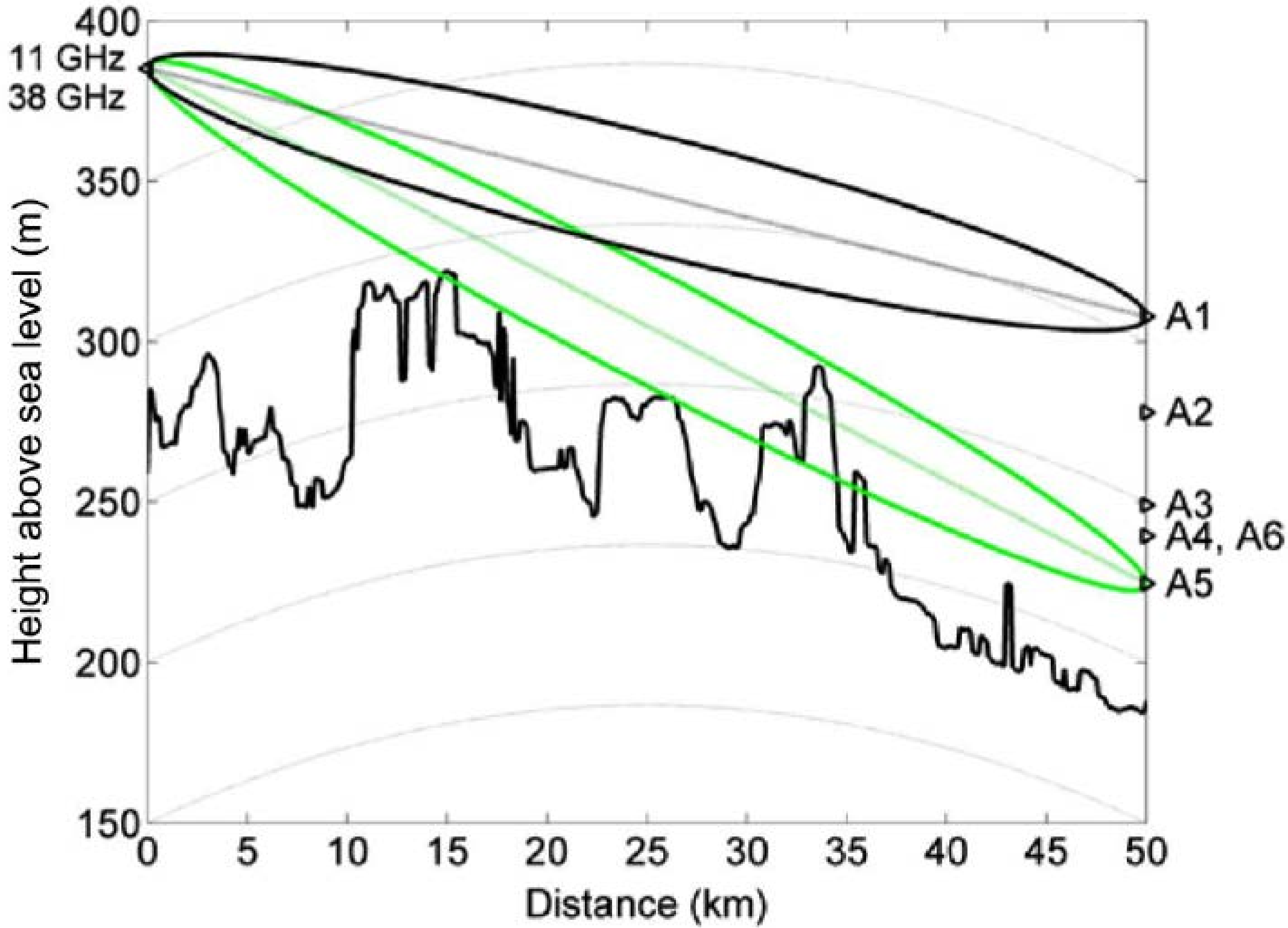
11 GHz
38 GHz
400
350
300
250
200
150
Height above sea level (m)
0
5
10
15
20
25
30
35
40
45
50
Distance (km)
A1
A2
A3
A4, A6
A5

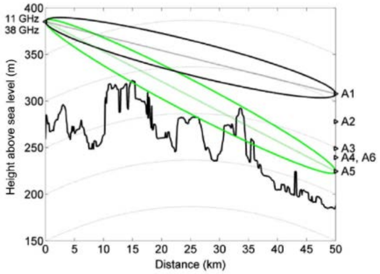
11 GHz
38 GHz
Height above sea level (m)
Distance (km)
A1
A2
A3
A4, A6
A5

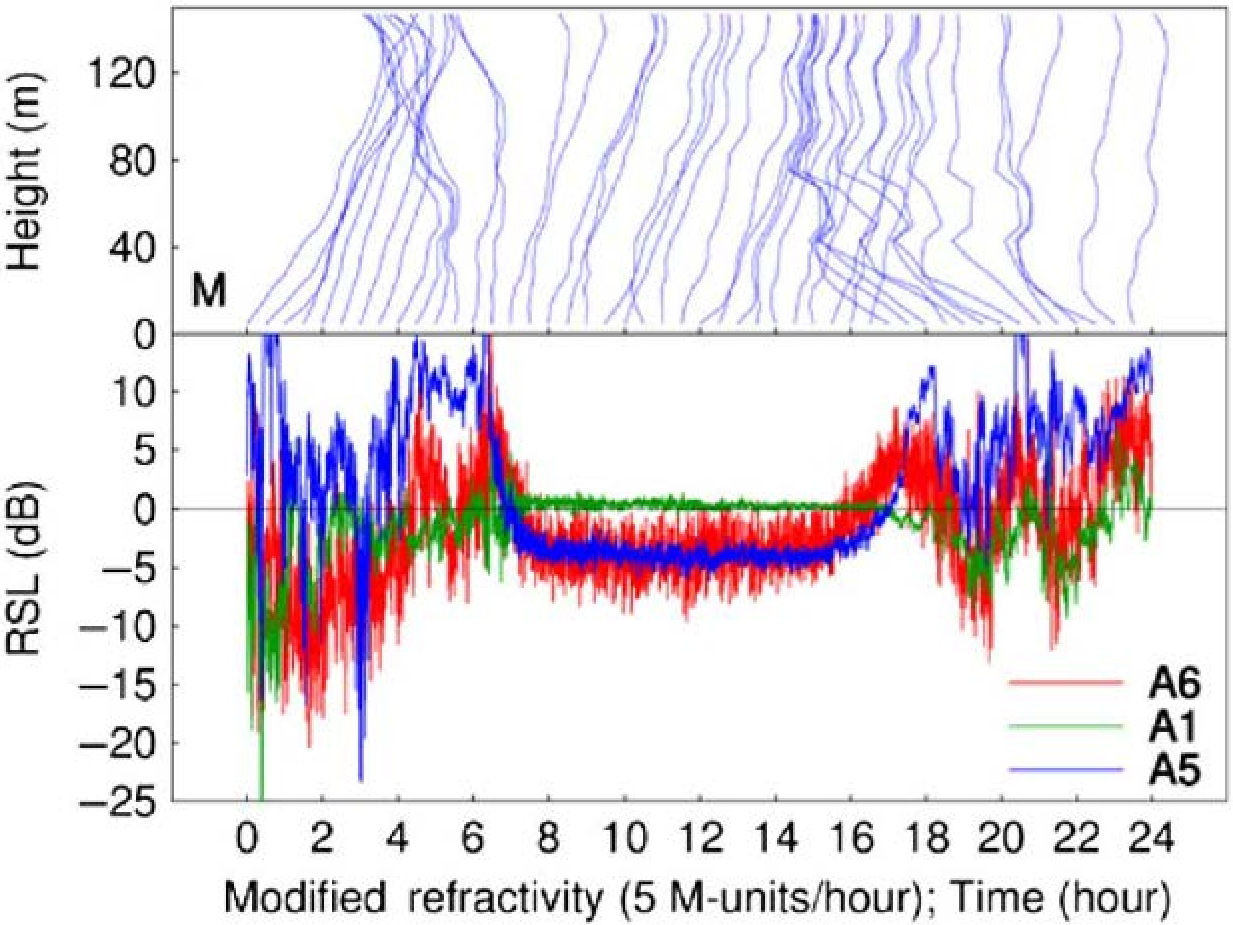
Height (m)
M
RSL (dB)
A6
A1
A5
Modified refractivity (5 M-units/hour); Time (hour)

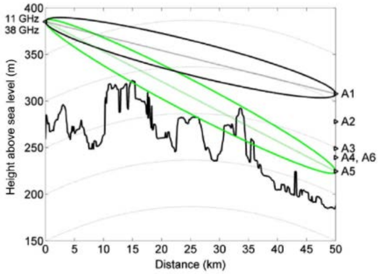


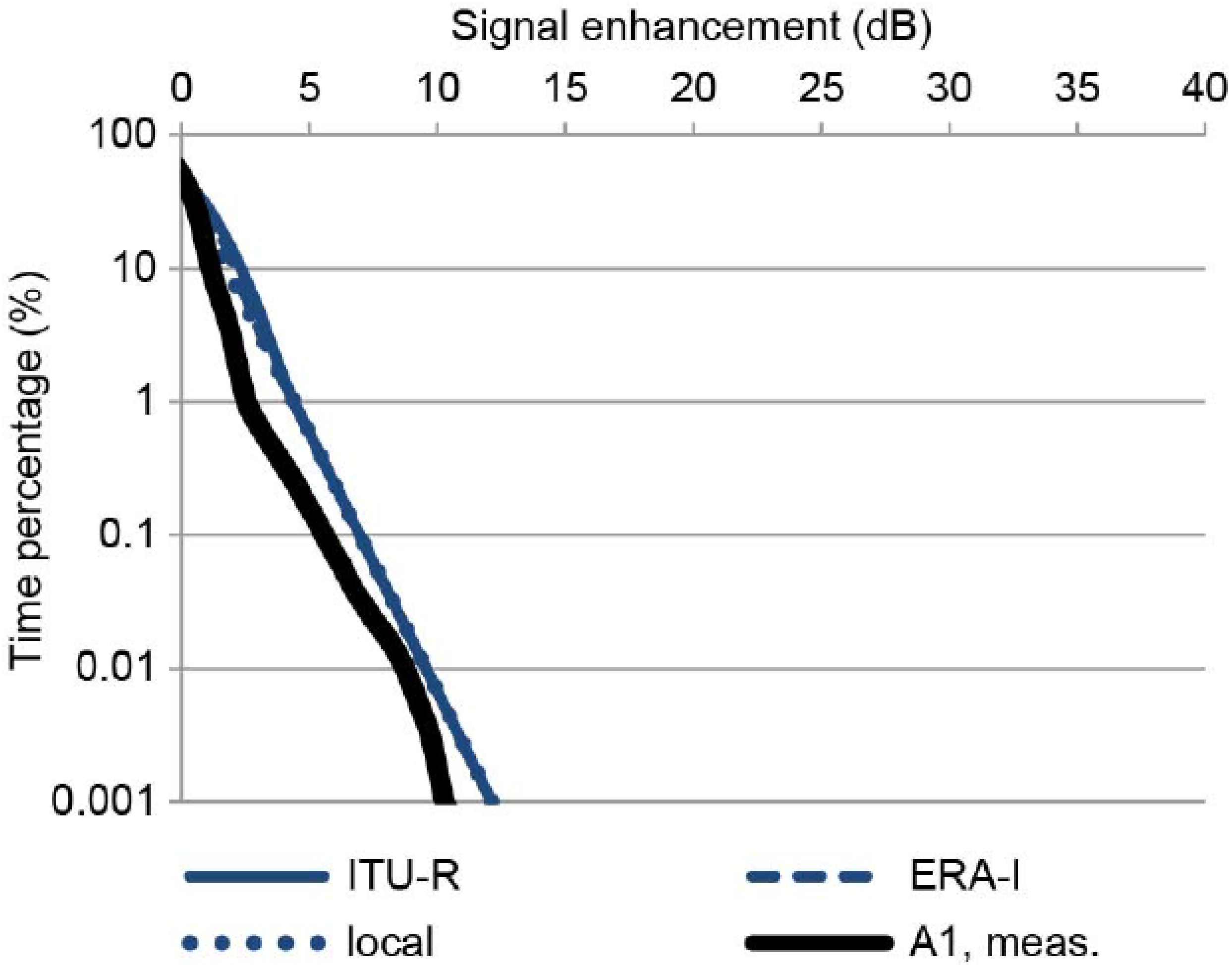


Fig. 6. 1-year statistics of signal enhancement and its prediction for channel A1.

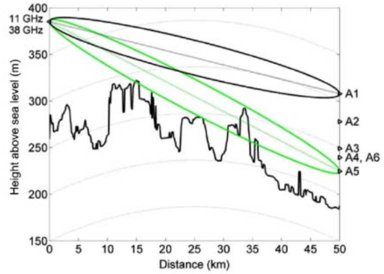
400
11 GHz
38 GHz
350
300
250
200
150
Height above sea level (m)
A1
A2
A3
A4, A6
A5
0
5
10
15
20
25
30
35
40
45
50
Distance (km)

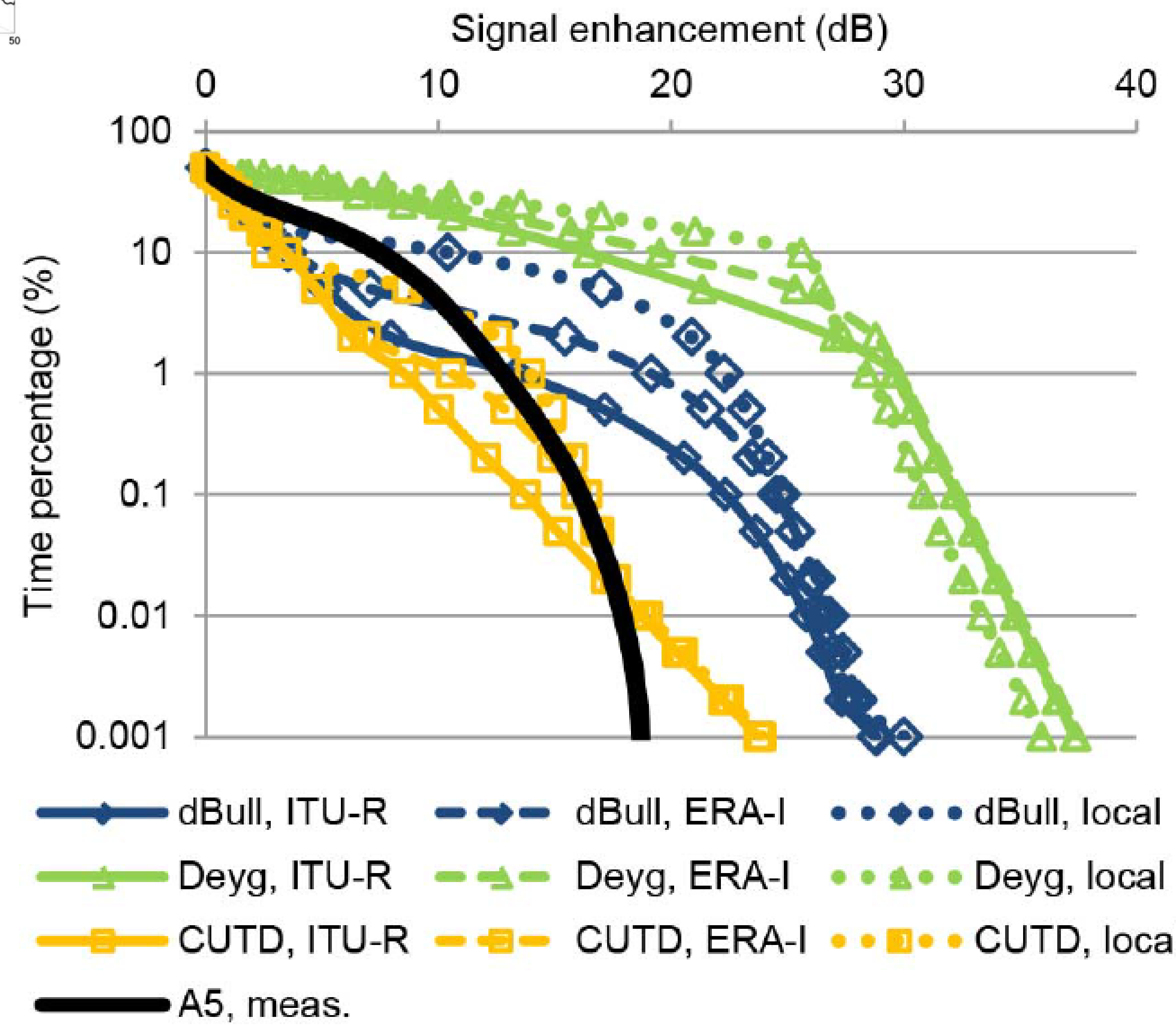
Signal enhancement (dB)
0
10
20
30
40
100
10
1
0.1
0.01
0.001
Time percentage (%)
dBull, ITU-R
dBull, ERA-I
dBull, local
Deyg, ITU-R
Deyg, ERA-I
Deyg, local
CUTD, ITU-R
CUTD, ERA-I
CUTD, local
A5, meas.

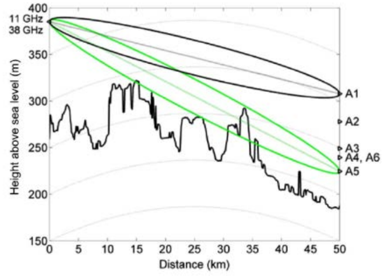

400
11 GHz
38 GHz
350
300
250
200
150
Height above sea level (m)
0
5
10
15
20
25
30
35
40
45
50
Distance (km)
A1
A2
A3
A4, A6
A5


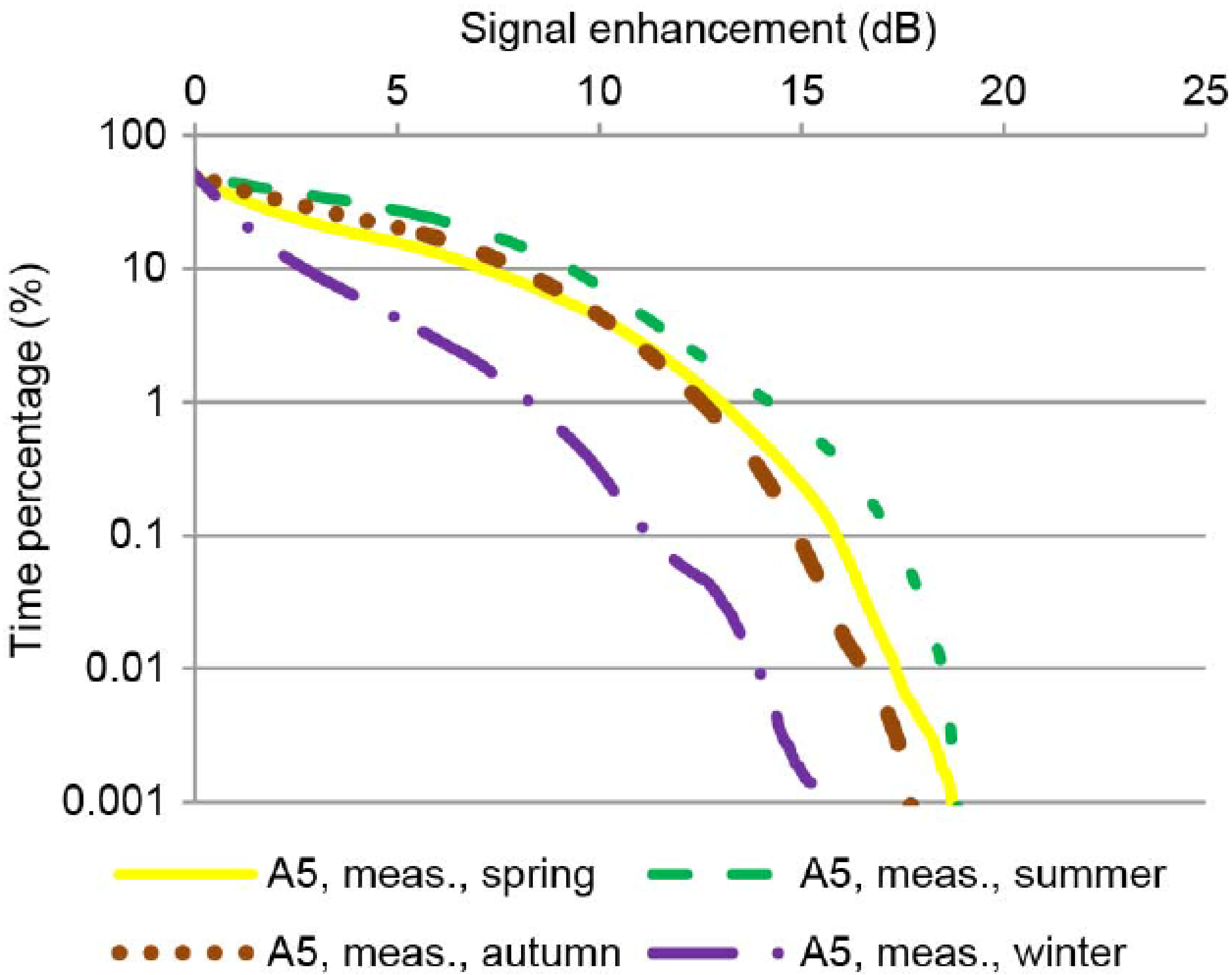

Signal enhancement (dB)
0
5
10
15
20
25
100
10
1
0.1
0.01
0.001
Time percentage (%)
A5, meas., spring
A5, meas., summer
A5, meas., autumn
A5, meas., winter

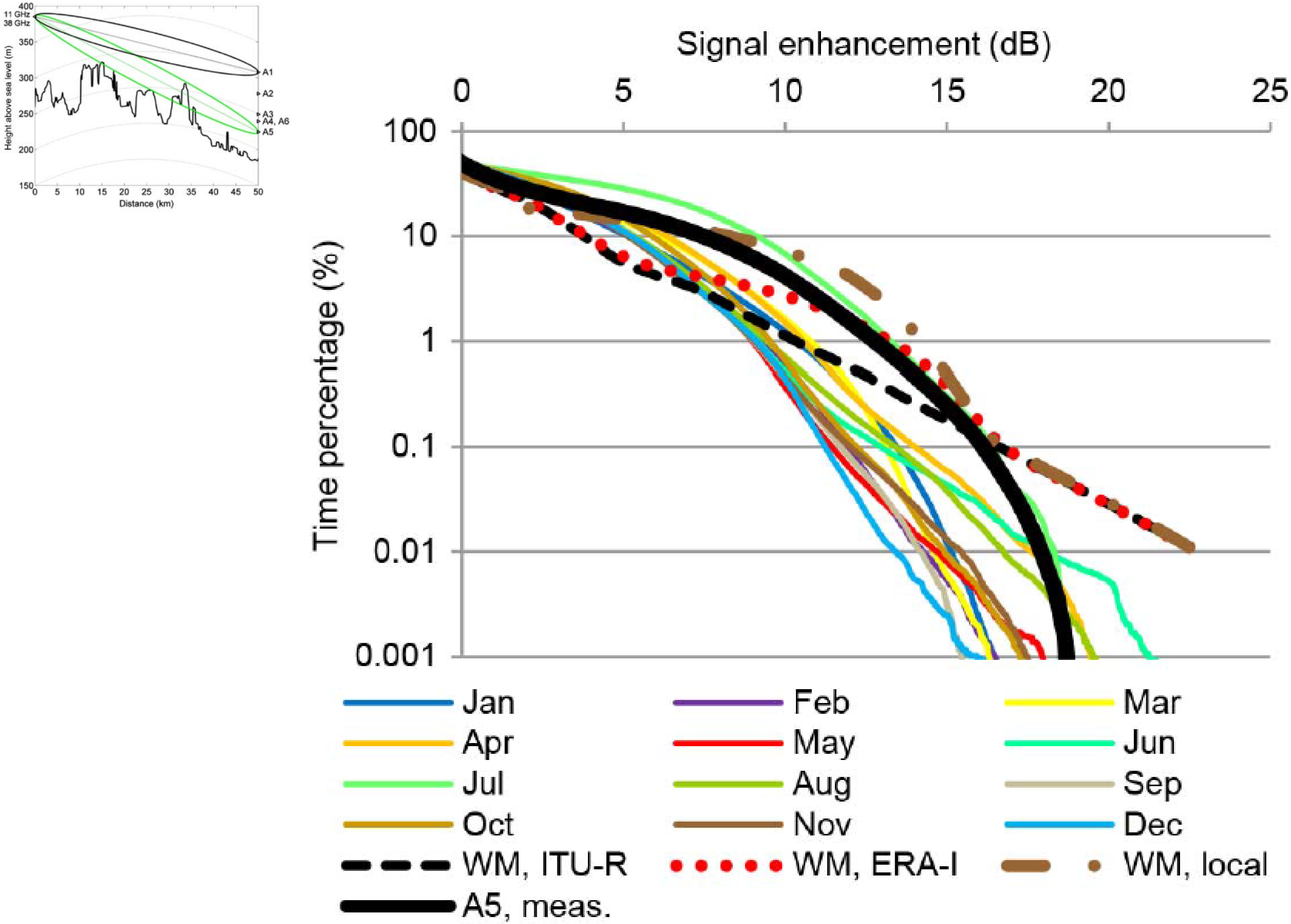


Fig. 10. Monthly statistics of signal enhancement for channel A5 and worst-month prediction considering the CUTD terrain diffraction method.